Spatially localized expression of glutamate decarboxylase gadB in Escherichia coli O157:H7 microcolonies in hydrogel matrix

Cedric Saint Martin, Nelly Caccia, Maud Darsonval, Marina Gregoire, Arthur Combeau, Grégory Jubelin, Florence Dubois-Brissonnet, Sabine Leroy, Romain Briandet, Mickaël Desvaux

Spatially localized expression of glutamate decarboxylase *gadB* in *Escherichia coli* O157:H7 microcolonies in hydrogel matrix

Cédric Saint Martin[1,2], Nelly Caccia[2], Maud Darsonval[1], Marina Grégoire[1], Arthur Combeau[1], Grégory Jubelin[2], Florence Dubois-Brissonnet[1], Sabine Leroy[2], Romain Briandet[1]* & Mickaël Desvaux[2]*

[1] Université Paris-Saclay, INRAE, AgroParisTech, MICALIS Institute, 78350 Jouy-en-Josas France,

[2] INRAE, Université Clermont Auvergne, UMR454 MEDIS, 63000 Clermont-Ferrand, France,

*Corresponding authors: M. Desvaux (mickael.desvaux@inrae.fr) & R. Briandet (romain.briandet@inrae.fr)

Abstract: Functional diversity within isogenic spatially organized bacterial populations has been shown to trigger emergent community properties such as stress tolerance. Taking advantage of confocal laser scanning microscopy combined with a transcriptional fluorescent fusion reporting at single cell scale the expression of the glutamic acid decarboxylase *gadB* in *E. coli* O157:H7, it was possible to visualize for the first-time spatial patterns of bacterial gene expression in microcolonies grown in a gelled matrix. The *gadB* gene is involved in *E. coli* tolerance to acidic conditions and its strong over-expression was observed locally on the periphery of embedded microcolonies grown in acidic hydrogels. This spatialization of *gadB* expression did not correlate with live/dead populations that appeared randomly distributed in the colonies. While the planktonic population of the pathogens was eradicated by an exposition to a pH of 2 (HCl) for 4h, mimicking a stomachal acidic stress, bacteria grown in gel-microcolonies were poorly affected by this treatment, in particular in conditions where *gadB* was spatially overexpressed. Consequences of these results for food safety are further discussed.

Keywords: *E. coli* O157:H7, food matrix, microcolonies, local gene expression, *gadB*, fluorescent transcriptional fusions, confocal laser scanning microscopy (CLSM), Food safety.

Abbreviations: CLSM: stands for "Confocal Laser Scanning Microscopy"; LMPA: stands for "Low Melting Point Agarose".

1) Introduction

Escherichia coli is a commensal bacterium found in the gut of mammals that plays an integral part in the digestive process. However, some strains of *E. coli* are pathogenic and represent a public health issue when they reach the production lines of food industries. Besides obvious evisceration accidents contaminating the meat at the slaughter state, food contamination of animal products (meat and milk products), vegetable or water usually occur through direct or indirect fecal contamination [1–3]. Storage conditions and holding temperature are then major contributors to bacterial growth and survival in food products [4]. Shigatoxin (Stx) encoding *E. coli* (STEC) are the third most common foodborne zoonosis in Europe [5] and amongst STEC, the serotype O157:H7 is a commonly identified agent in patients. *E. coli* O157:H7 are enterohaemorrhagic *E. coli* (EHEC) responsible for bloody diarrhea when the intestinal lining is broken by the presence of Stx. A possible outcome of Stx passing in the bloodstream is damage to the kidneys that can lead to a hemolytic uremic syndrome (HUS), which itself lead to fatal outcomes in 5% of cases [6]. Children are especially at risk and *E. coli* O157:H7 is still the main cause of pediatric HUS [7]. At the level of the European union, regulations ask for the absence of this pathogen in 25g of germinated seeds (Regulation CE 209/2013, amendment 2073/2055), but no equivalent exist for meat products. Precautionary measures for meats exist at a state level in the Union (France, DGAL/SSDSA/2016-353). However, the pathogen is still routinely detected at levels above 100 CFU/g in more than 1% of all red meats, the main vector of infection for this pathogen [5,8].

Structured food matrices are a continuity of heterogeneous local microenvironments harboring multiple micro-gradients that can evolve with time and microbial activity [9]. This leads bacterial cells in food matrices to face different biotopes in which their growth and behavior can diverge from observations in liquid laboratory media. Therefore, environmental conditions of food matrices can prompt high phenotypic diversity in microbial populations as the cells adapt to local microenvironments [10,11]. In comparison with their planktonic counterparts, phenotypic diversity in structured communities can influence bacterial fitness and behavior, such as increase expression of virulence genes [12], higher tolerance to antimicrobials agents and thermal stress [13,14], or improved cell motility [15]. While several

studies reported emergent properties of bacterial community in food matrices at the population level [13,16–19], no experimental evidence has yet been reported on the spatial heterogeneity of gene expression at the scale of single cells.

The stomachal phase after food ingestion exposes bacteria to strong acidic pH conditions for several hours and is credited for the highest population reduction of the bacterial load. High tolerance to acidic conditions is therefore necessary for foodborne pathogens, and involved systems that regulate intracellular pH. The glutamic acid decarboxylase (GAD) is one among various systems of acid resistance (AR) commonly found in bacteria able to survive in extreme acid conditions [20–24]. In *E. coli*, the GAD system is a three components system: two glutamate decarboxylases, GadA and GadB, which use cytoplasmic free protons by converting glutamate into γ-aminobutyrate (GABA), and the glutamate/GABA antiporter GadC. When the pH is below 5.6, cytoplasmic GadB migrates near the inner membrane to maximize collaboration with transmembrane GadC [25]. While *gadA* is independent in chromosomic location and *gadB* and *gadC* are organized in operon, the expression of both *gadA* and *gadBC* is transcriptionally regulated by RpoS, two AraC-like regulators GadX and GadW, and by effectors with two inhibitors, the cyclic AMP receptor protein and H-NS. H-NS and RpoS in particular determine the temporal expression, the former inhibiting *gadB* expression, whereas RpoS promotes the transcription of *gadB* once the stationary phase is reached [26].

To decipher and model fitness and behavior of *E. coli* O157:H7, synthetic microbial ecology approaches were used in structured food matrices where the complexity of the communities and the factors of influence are reduced to their minimum, but increased in their controllability [27]. Such approaches have been used to describe how matrix parameters affect bacterial growth and morphodynamics of microcolonies [16,28]. In a recent contribution, we have shown that the volume, distribution and sphericity of microcolonies of *E. coli* O157:H7 in hydrogel are dependent of the size of the inoculum, but also on the concentration of acids and NaCl, two environmental stresses frequently encountered in food products [29].

In this study, we took advantage of a hydrogel matrix to observe the local expression of *gadB* in *E. coli* O157:H7 cells in microcolonies using confocal laser scanning microscopy (CLSM). To explore the existence of patterns of expression in microcolonies, bacterial strains with a dual transcriptional fluorescent reporter system were engineered to monitor the spatial expression of *gadB* at the single cell scale. In order to relate the impact that phenotypic heterogeneity in microcolonies can have on community function, the survival of

planktonically grown cells to a strongly acidic media mimicking the stomachal passage was further assessed and compared to cells grown or dispersed in hydrogels.

2) Material and methods

Bacterial strains and culture conditions

From cryotubes stored at -80°C, the bacterial strain of *E. coli* (see genetic construction) was plated on Petri dishes with TSA (Tryptone Soya Agar, Oxoid, USA) and incubated overnight at 37°C. One bacterial colony was picked up and inoculated in TSB (Tryptone Soya Broth, Oxoid, England) before overnight incubation at 37°C under orbital shaking (200 rpm). When required, growth media were supplemented with chloramphenicol (Cm 25 µg/mL; EUROMEDEX, China). The strain *Lactococcus lactis* ssp. cremoris (Aerial N°2124) was incubated in the same conditions, but without antibiotic supplementation.

Genetic construction

The *E. coli* O157:H7 CM454 [30,31] is the wild type strain in this study. We used a T7 polymerase (T7pol) amplification technique inspired from previous reports [32,33], where the cassette *T7pol::Cm*^{R} is inserted after the genetic sequence of the gene *gadB* using the Datsenko-Wanner [34] recombination technique (supplementary material Figure S1). Regions of identity were added at the ends of the cassette by the forward primer: 5'CCGAAACTGCAGGGTATTGCCCAACAGAACAGCTTTAAACATACCTGATAACA GGAGGTAAATAATGCACACGATTAACATCGC3' and reverse primer: 5'AAATTGTCCCGAAACGGGTTCGTTTCGGACACCGTTACCGTTAAACATGGAGTT CTGAGGTCATTACTG3'. The correct insertion of *T7pol::Cm*^{R} in the construct was verified by PCR using the forward primer 5'GGAAGACTACAAAGCCTCCC3' and reverse primer 5' TATTCCTGTCGGAACCGCAC3', for sequencing (Eurofins Genomics, Germany). Based on the sequence of the pHL40 plasmid [32], a new plasmid was synthetized (GeneArt, ThermoFisher Scientific, Germany) bearing the P_{T7pol}*::GFPmut3::*T_{p7pol} as a GFP reporter but modified by insertion of P_{BBa_J23119}*::mCherry2::*T_{BBa_B0062} (iGEM parts) for constitutive expression of a red fluorescent protein (RFP). This new plasmid, called pHL60, was transformed into competent *gadB::T7pol::Cm*^{R} bacterial cells. This system is an indirect reporter of *gadB* transcription as the transcriptional fusion of *gadB::T7 polymerase* allows an amplified production of GFP (GFPmut3) from pHL60 and normalization of the level of expression respective to the constitutive expression of the RFP (mCherry2) from the same plasmid, to minimize variations of the fluorescence associated with variations in the number

of plasmids from one cell to another. To validate the genetic construction, the reporting planktonic expression of *gadB* was tested on six pH values from 4.5 to 7.0 using a microplate reader (Synergy H1, Biotek) (Supplementary material Figure S2).

Transparent hydrogel matrices for fluorescent imaging

As previously described [29], the hydrogel matrices were obtained by mixing TSB with 0.50 % low melting point agarose (LMPA) (UltraPure Agarose, Invitrogen, USA). After boiling, the liquid LMPA at neutral pH (pH=7) was cooled down to 40°C to prevent thermal stress before the bacterial inoculum was added to obtain 10^4 CFU/ml. When necessary, the medium was adjusted to acidic pH= 5 with HCl. After homogenizing and gentle stirring to avoid bubble formation, the inoculated gel matrix was immediately distributed in each well of a 96-well microtiter plate of microscopic grade (µClear, Greiner Bio-One, France). The microtiter plates were then incubated at 20°C and observed under CLSM after 96 hours of incubation.

All microscopic observations were performed with a Leica HCS-SP8 confocal laser scanning microscope (CLSM) at the INRAE MIMA2 imaging platform (https://doi.org/10.15454/1.5572348210007727E12). The GFP (GFPmut3; λ_{ex}500; λ_{em}513) and RFP (mCherry2; λ_{ex}589; λ_{em}610) were excited respectively with laser bands 488 nm and 561 nm. For Live/dead exploration, SYTO9 (λ_{ex}485; λ_{em}501) and IP (λ_{ex}535; λ_{em}617) were excited respectively with laser bands 488 nm and 561 nm. Observations were carried out with a water immersion 63x objective lens (numerical aperture of 1.20) for 184µm x 184µm fields. Bidirectional acquisition speed of 600 Hz allows a frame rate of 2.3 images per second. For 3D stack analysis, a 1 µm step between z levels was used. For each condition, a minimum of 60 stacks were acquired in over a dozen independent wells. Microscopic images were treated on IMARIS v9.64 (Bitplane, Switzerland) to generate sections and projections. Kymograms reporting the spatial analysis of *gadB* expression in microcolonies were performed using BiofilmQ v0.2.2 [35]. BiofilmQ image segmentation was performed with a threshold value set at 0.1 with cubes of 1.8 µm (vox of 10). The absence of radial fluorescence gradients in microcolonies of *E. coli* O157:H7 constitutively expressing GFP was verified prior experiments with *gadB* expression (supplementary material Figure S3).

Acidic digestion challenge

To test the ability of *E. coli* O157:H7 population to survive the strong acidic stress during the stomachal passage, 3 ml of planktonic cells (TSB), planktonic cells grown in TSB and then encased in gel matrix (TSB-LMPA) or gel-colonies cultures (LMPA) (72h, 20°C, pH=7 or

pH=5) were transferred in 27 ml of NaCl 9g/L saline solution (control groups) or 27 ml of a saline solution adjusted with HCl (5 M) to a pH of 2. The cups were then incubated at 37°C for 4 hours under a 90-rpm shaking to simulate matrix digestion. All media were then homogenized to disperse bacteria (IKA Ultra-Turrax T25; Janke Kunkel) and the resulting suspensions were immediately plated on agar for enumeration and determination of the log reduction in CFU/ml before and after acidic treatment.

Statistics

Graphics and ANOVA variance analysis were performed with Prism 9 (GraphPad; CA, USA). Differences were considered significant when $P<0.05$ with P being the critical probability associated with the Fisher test.

3) Results

Spatial patterns of gadB expression in gel-microcolonies

Mean radius of microcolonies grown in neutral or acidic hydrogel showed little differences between neutral (28 µm) and acidic conditions (27 µm), the repartition of populations around these values was noted to not be statistically significant (Figure 1, obtained from measurement on 40 colonies, $P>0.05$). However, at pH 5, microcolonies appear more circular than at pH = 7 and they harbor at their edge a streamer population shedding from the colony core, forming a crown around it (Figure 2).

Microscopic observations of the fluorescence reporting the expression of *gadB* in cells inside microcolonies (Figure 2) show radically different patterns between the two hydrogels. In neutral pH conditions, the gene is expressed at a basal level throughout the whole microcolony with no specific spatial arrangement (Figure 2A, supplementary material Figure S4). By contrast, the expression of *gadB* is strongly overexpressed in the periphery of the colonies formed in acidic hydrogel (Figure 2B, supplementary material Figure S4). Those qualitative observations were reinforced by a quantitative exploration of the radial distribution of *gadB* expression (Figure 3). For both hydrogels, the genetic expression is monitored by the green fluorescent intensity normalized with the red constitutive fluorescent intensity. 3D kymographs integrating 40 independent microcolonies (X-axis) for each condition represent in color code *gadB* transcription from the center of the microcolony (Y-axis, d_{CM}=0 µm) to

188 the edges of the colonies and beyond. Where in neutral pH hydrogel *gadB* expression is low
189 and almost constant over the radius of the microcolonies (Figure 3A), acidic hydrogels
190 present a sharp band of *gadB* over-expression in between 25 and 30 µm from the center of the
191 microcolonies (Figure 3B). This is consistent with the observed spatial expression as the
192 radius of the microcolonies is 27-28 µm (±5 µm) in these experimental conditions.
193 Interestingly, when microcolonies merge as they grow, they behave like a single colony in
194 regard to the peripheral *gadB* spatial expression. Similarly, if two microcolonies are in near
195 contact, the two sides facing each other do not present an over-expression of *gadB* or the
196 shedding of single cells visible in other areas of the periphery (supplementary material Figure
197 S5).

198 Control experiments performed with a constitutive expression of the green fluorescence
199 protein did not show the spatialization of the expression as presented above (supplementary
200 material Figure S3). A time-course microscopic analysis allows the observation of *gadB*
201 expression spatialization in acidic hydrogels as early as microcolonies become visible under
202 the microscope, ~48h after inoculation (data not shown). Finally, the spatial repartition of
203 dead cells in gel-microcolonies as shown by live/dead fluorescent staining indicated a random
204 distribution of the red dead cells, with no preferential localization in the microcolonies
205 associated with cells expressing *gadB* (supplementary material Figure S6).

206 Following those results, *E. coli* O157:H7 was then cultured in the presence of *Lactococcus*
207 *lactis* ssp. *cremoris* (Figure 4). The ability of *L. lactis* to produce *in-situ* lactic acid is used to
208 replicate the natural acidification of food matrix containing *L. lactis* (cheese), or where a
209 progressive accumulation of lactic acid occurs (meat). Exploration of the hydrogel was
210 performed 72-96h after inoculation. Contrary to observations where lactic acid is added in the
211 hydrogel preparation [29], microcolonies of *E. coli* O157:H7 are present and possess the same
212 morphology as seen in mono-cultures in the acidic condition (Figure 4A). Close up on 50 µm
213 thick slices of microcolonies of *E. coli* O157:H7 in close proximity to microcolonies of *L.*
214 *Lactis* clearly shows the same spatial patterns of *gadB* expression as previously encountered
215 for the mono-cultures in acidic media (Figure 4B).

216

217

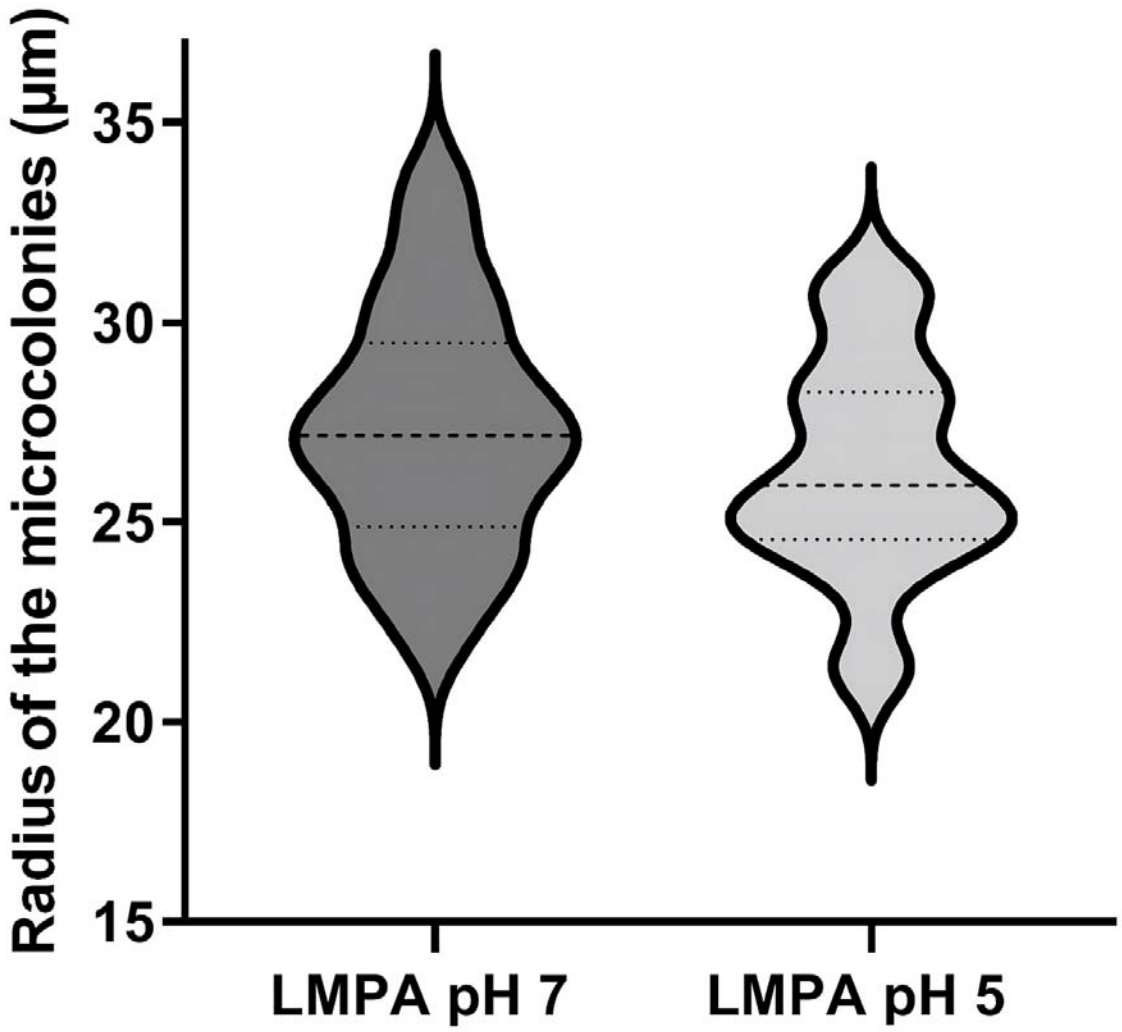

Figure 1: Radius of the microcolonies. Representation of the radius of the microcolonies in µm, the width of each figure represents the concentration of the number of values. For each case, the slashed line is the mean value of radius, and dotted lines delimit the 75 % probability interval. Radius values were calculated from 40 independent microcolonies.

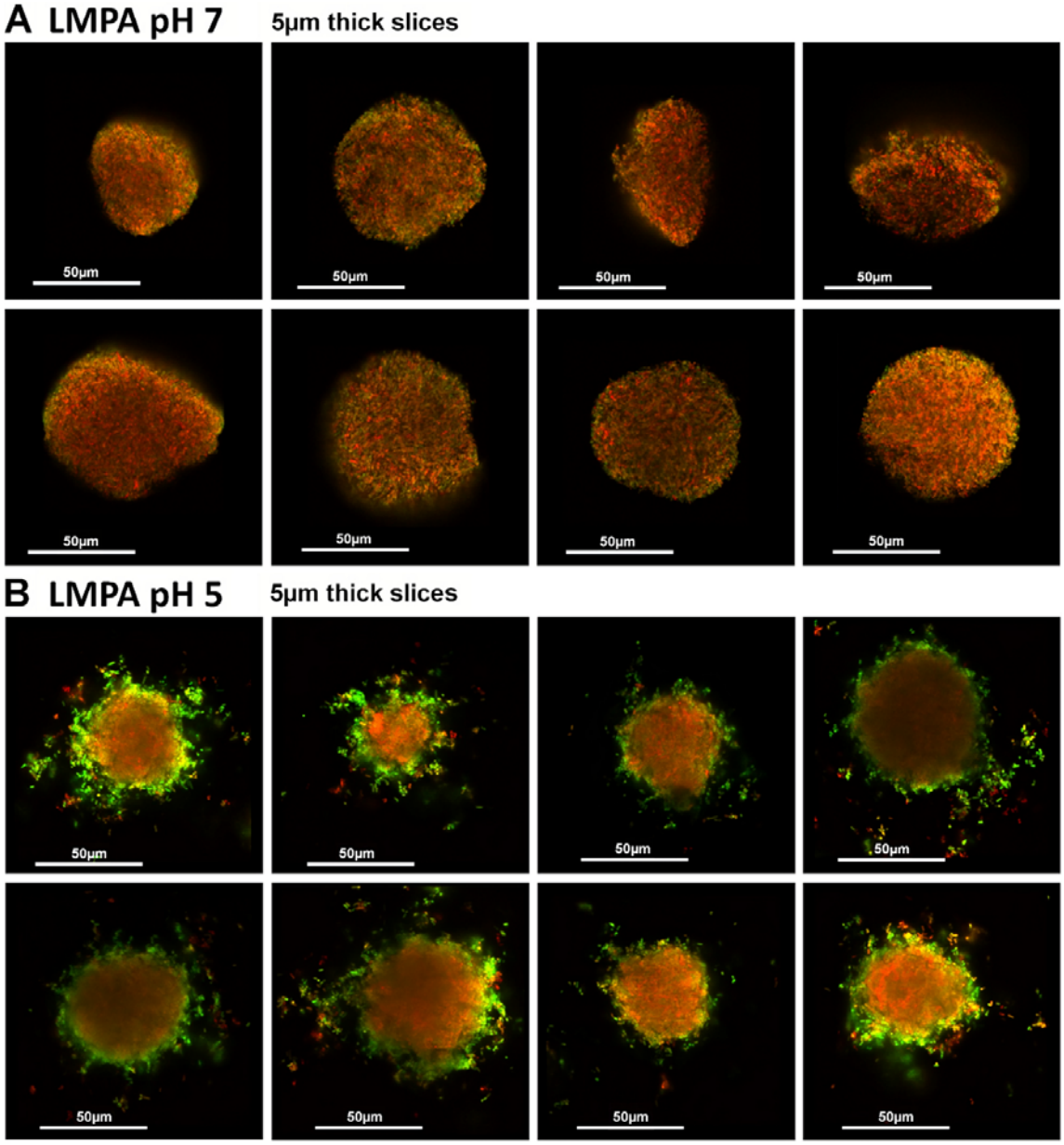

Figure 2: Representative images of *gadB* spatial patterns of expression for *E. coli* O157:H7 cultivated in neutral (pH=7) or acidic (pH=5) hydrogels. A series of 5µm slices of microcolonies is presented in control LMPA pH=7 (A) and the acid matrix LMPA pH=5 (B). The red fluorescence is constitutive and the green fluorescence is expressed as a function of *gadB* transcription. Supplementary material Figure S3 presents the same representation for a control constitutive GFP expression in both conditions.

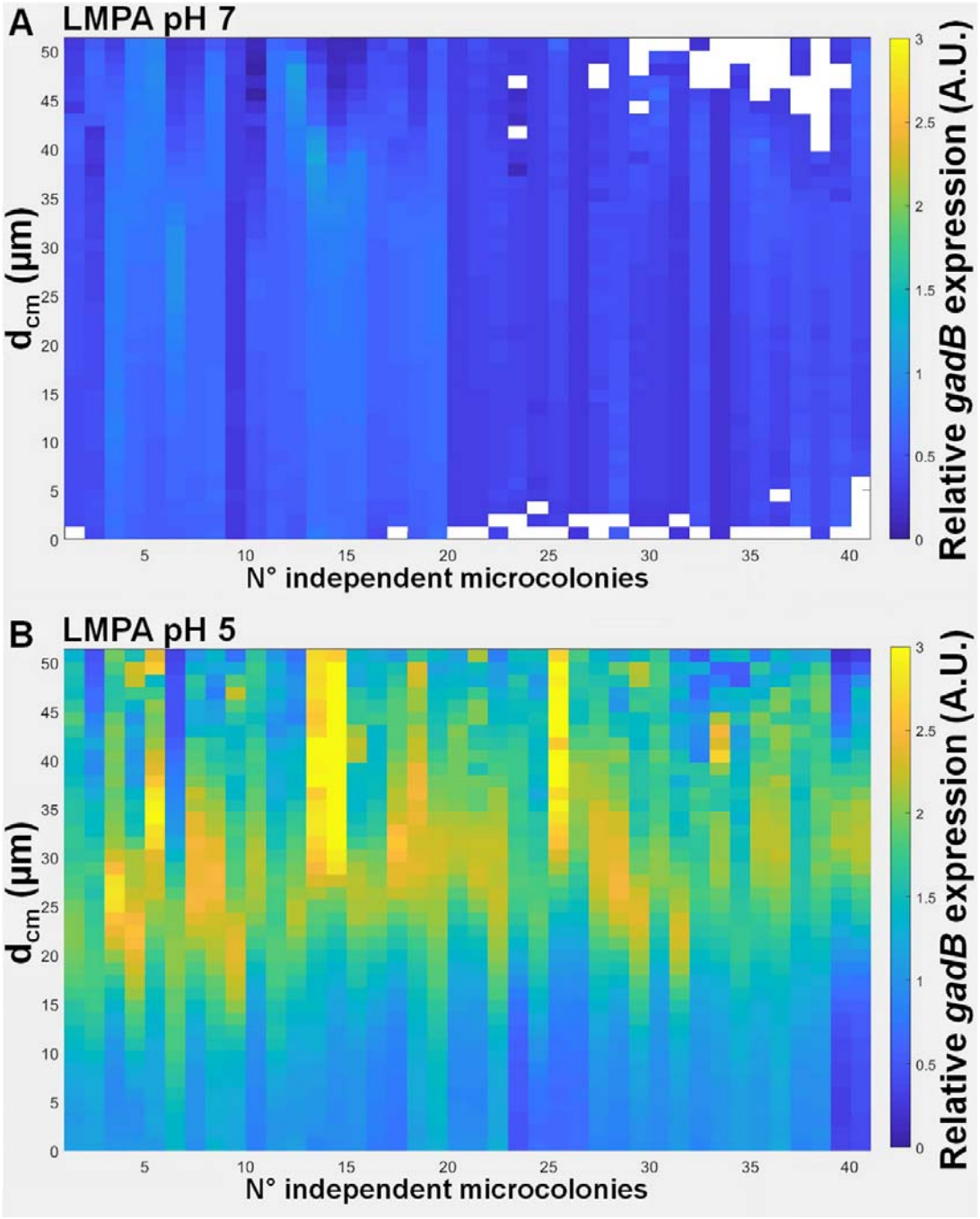

Figure 3: Relative expression of *gadB* in function of the distance from the center of microcolony. In this representation, the relative *gadB* expression is expressed as the ratio of green fluorescence intensity over red fluorescent intensity (GFP reporter/RFP constitutive) in function of the distance from the center of the microcolony (d_{CM}) for forty microcolonies grown in neutral (A) or acidic hydrogels (B).

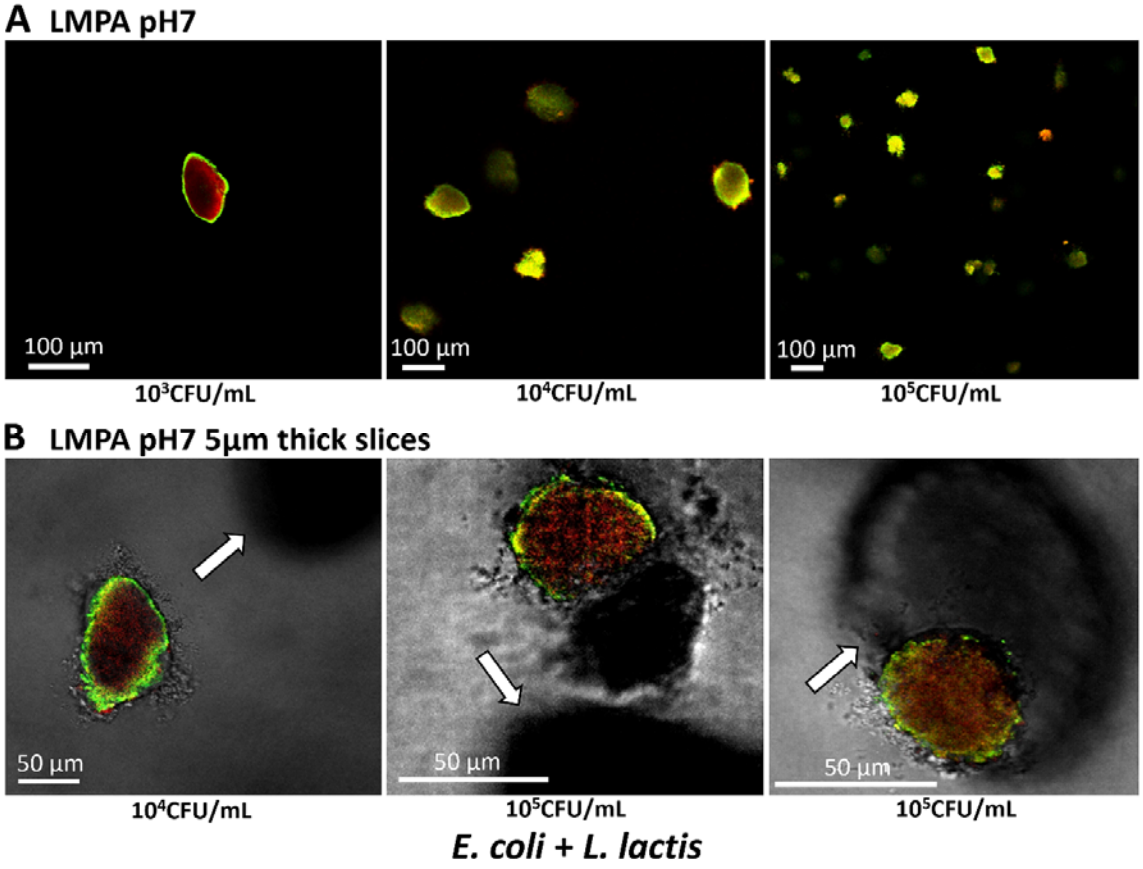

Figure 4: Spatial patterns of expression of *gadB* for *E. coli* O157:H7 in the presence of *Lactococcus lactis* ssp. *cremoris*, cultivated at neutral pH in hydrogels. (A) Visualization at 96h of microcolonies of *E. coli* O157:H7 co-inoculated from 10^3CFU/ml to 10^5CFU/ml, with *L. lactis* inoculated at 10^3CFU/ml, in a hydrogel at neutral pH. The red fluorescence is constitutive and the green fluorescence is expressed as a function of *gadB* transcription. (B) Microcolonies of *E. coli* O157:H7 close or in contact with *L. lactis* microcolonies. The two rightmost pictures were taken at 96h and the one on the left at 72h. *L. lactis* microcolonies are visualized in the bottom images thanks to the transmission detection (indicated by white arrows).

Increased survival to acidic stomachal stress of E. coli grown in gel-microcolonies

As the capacity of survival to stomachal acidic stress of *E. coli* O157:H7 populations is of interest for public health safety, the acid resistance of bacteria grown planktonically or in hydrogel matrices was evaluated by enumeration on agar after acid stress.

Cultures of *E. coli* O157:H7 adjusted to 10^4 CFU/ml were incubated at neutral (pH=7) or acid pH (pH=5) in either TSB or LMPA. After 96h of incubation at 20°C, the populations reached values of log CFU/ml of 9.4/9.6 in TSB at pH neutral/acid and 9.5/8.6 in LMPA at pH neutral/acid.

Bacteria grown in planktonic conditions (TSB) were highly sensitive to the 4-hours exposition to pH=2 with a total loss of the culturable population (9 log reduction) (Figure 5). In contrast, cells grown as spatially organized colonies in LMPA for 96h presented a statistically high tolerance to this strong acidic stress ($P<0.05$). The best tolerance was observed for the microcolonies incubated at a pH of 5 with a log reduction as low as 0.29 log CFU/ml, statistically significantly lower than the reduction observed for microcolonies incubated at neutral pH, where the log reduction is 0.78 CFU/ml ($P<0.05$). To test for interferences of the hydrogel to bacterial acidic stress, planktonic populations cultivated in TSB were encased in LMPA just before the survival test. Log reduction of these control planktonic populations suspended in LMPA presented significant similar sensitivity than planktonic TSB culture ($P>0.05$), indicating no buffering effect of agarose to stomachal acidic stress.

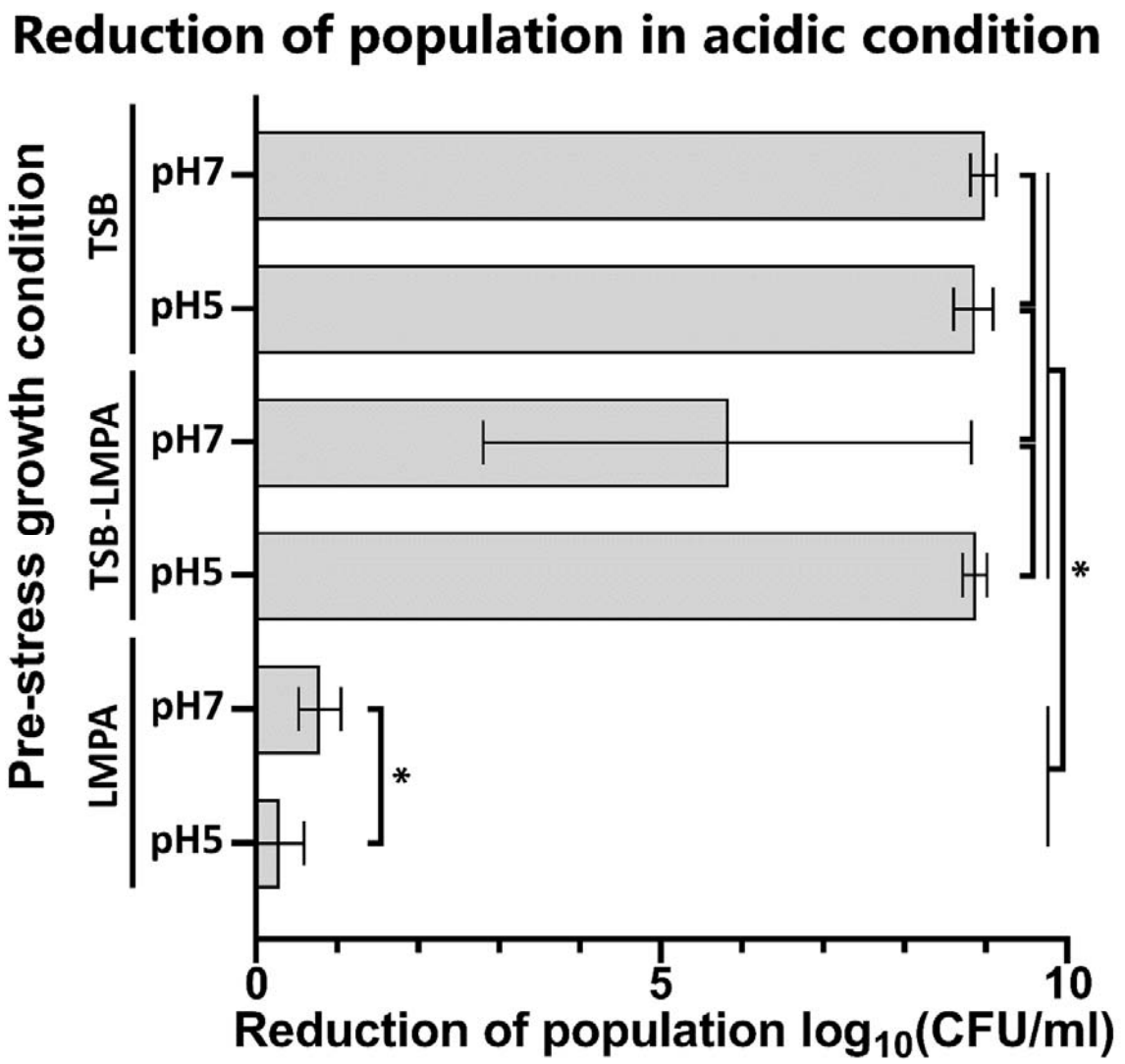

Figure 5: Population log- reduction of planktonic cultures and hydrogel microcolonies of *E. coli* O157:H7 upon acidic exposure. Bacterial cells were exposed for 4 hours at a pH of 2 (HCl). Representation of the mean reduction of population log between the control and survival groups. Bacteria incubated and tested in planktonic are on the top (TSB), those incubated in planktonic but encased in hydrogels before the test are on the middle (TSB-LMPA), and the results for populations incubated and tested in hydrogels are on the bottom (LMPA). A star indicates a significant difference between values (P<0.05). Data resulted from at least six biological replicates**.**

4) Discussion

The behavior of microbial population in laboratory liquid growth media can strongly deviate from what is observed in real solid food matrices [18,36–40]. The environmental heterogeneity of structured media is listed as one of the four main causes of cellular variation, among genetic variation, aging and stochasticity of gene expression [41]. As such, it can trigger a large diversity of phenotypic cell expression in the same biotope, promoting the cohabitation of cells with different spectra of behaviors, such as stress response or virulence [42,43]. Structured food are not an optimal medium from an exploration perspective as the opacity of numerous food matrices prevents live imaging and microscopic approaches. To overcome these limitations, several studies take advantage of synthetic hydrogelled systems to simplify and control the parameters of growth of embedded bacteria. Here, low melting point agarose is used as a gelling agent in which cells can be dispersed without thermal stress and with tunable textures and media compositions. Thus, in a recent contribution, we have been able to mimic the texture of various food environments such as grounded meat or cheese [29]. The experiments presented in this work show that the morphology of microcolonies in the media complemented with HCl are different from the neutral pH control, in particular bacteria are shedding from the periphery of the microcolonies. This effect can be explained by a combined action of relaxed gel structures due to low pH and the higher motility of *E. coli* O157:H7 when acidic conditions are encountered [29,44].

In this study, we observed a clear overexpression of *gadB* for a subpopulation of cells localized in the periphery of microcolonies formed in acidic hydrogels. This gene is overexpressed at levels 2-3 times higher than in neutral conditions, which is in accordance with results obtained in planktonic conditions (Supplementary material Figure S2). We confirmed that this spatialization was neither associated with dead cells (supplementary material Figure S6), nor a limitation of oxygen for GFP maturation in the center of the microcolony (supplementary material Figure S3). The use of a single plasmid bearing both the genes for the constitutive and induced fluorescence means that, at the image analysis step, we prevented bias due to differences in plasmid copy numbers or differences in coloration from a mix of dye/genetic reporters [45]. The use of two lasers with different properties of matrix penetration could lead to a bias in the Z axis, but 3D analysis of all the cells in a microcolony reduces the bias as any offset at the bottom of the agglomerate is compensated by an opposite offset at the top.

Spatial patterns of genetic expression were previously reported for other genes in other bacterial species in surface biofilms either on solid or liquid, such as localized expression of *E. coli* sigma factors and type 1 pili, as well as *Pseudomonas aeruginosa* β-lactamase in biofilms [46–48]. To our knowledge, such patterns of gene expression were never reported in food or hydrogel matrices. Last experiments of co-cultures of *E. coli* O157:H7 and *L. lactis* demonstrate that the pattern of *gadB* expression could naturally occur in food matrix through a progressive accumulation and diffusion of lactic acid in the media, such as in cheese or meat products.

Then, we explored the consequences of growing populations in a structured media in regards of survival to an exposition to low pH media. Results showed that, regardless of the initial pH, populations incubated in a semi-solid media have a better tolerance to acid stress than those grown in liquid broths, where no surviving cells were detected. This underlines limitations in modeling food-borne pathogens behavior in food from data obtained in liquid conditions, as previously shown in other studies[18,36,37,49].

It has been suggested from other studies that the components of the matrix could have a buffer effect that protects embedded cells by preventing the drop in pH. Our tests show that planktonic populations dispersed in hydrogel did not present the same survival fitness that those cultivated as microcolonies in the same hydrogel. The hypothesis of a buffer effect due to hydrogel interference was tested for bacteria incubated in hydrogel and it was statistically rejected. This is supported by another study in a gelified dairy matrix, where food related bacteria were dispersed without incubation in the gel before application of the acidic stress. It was reported that no protective effect existed compared to the same conditions in liquid media [50].

A parameter that could explain this difference of survival between the populations incubated or not in the hydrogels would be the spatial organization of cells. The hydrogels showed evidence of deliquescence such as unraveling of filaments and loss of stiffness but maintained enough structural integrity to ensure the microcolonies did not disperse. The ability of spatially organized populations of bacterial cells to better survive acid stress was described for pathogenic bacteria but also for auxiliary microbiota and probiotics, such as *Lactobacillus* strains [51,52]. The bacteria could secrete extracellular polymeric substances (EPS) when grown in communities as described in biofilms [53,54]. For *E. coli* O157:H7, tolerance of the bacteria to low pH could further involve the DNA binding protein Dps which is known to enhance survivability when local nutrients are exhausted [55,56].

From this study in a hydrogel matrix, *gadB* appeared to be more expressed at the periphery of the *E. coli* O157:H7 microcolonies in acidic conditions. This correlated with an increased tolerance to the type of acid stress that can be encountered by bacterial cells after ingestion of food. These findings are of interest for public health as they underline possible differences between liquid and solid food products on the infectious dose and bacterial virulence. In this case, the tolerance to acidity could mean an increase in the bacterial load that can survive in the digestive system as well as a phenotype more likely to colonize the gut lining. In order to alleviate public health issues, differences in bacterial behavior in planktonic conditions versus microcolonies could be considered when integrating phenotypic heterogeneity in risk assessment. Modeling pathogens growth and survival should take in account the gelled environments where the spatialization of genetic expression and its resulting populational effects could deeply affect pathogens behavior and virulence after ingestion.

Declaration of competitive interest

None

Acknowledgments

This work was supported in part by INRAE and ANR (Agence National de la Recherche) PathoFood project (n°ANR-17-CE21-0002). The partners of the ANR PathoFood are acknowledged for fruitful discussions about *L. monocytogenes* and *E. coli* O157:H7 behavior in food matrices. Cédric Saint Martin was a PhD Research Fellow granted by the ANR PathoFood. Julien Deschamps (INRAE) is warmly acknowledged for assistance with Confocal Laser Scanning Microscopy at the Mima2 imaging platform (https://doi.org/10.15454/1.5572348210007727E12).

Author contributions

CSM, RB and MD, conceptualized the overarching aims of the research study. CSM, NC, MD, MG, AC, GJ, FDB, SL, RB and MD conceived and designed the experiments. CSM, NC, MD, MG and AC performed the experiments and data acquisition. CSM, NC, MD, AC, GJ, FDB, SL, RB and MD analyzed and interpreted the data. RB and MD had management as well as coordination responsibility for the execution of the research work. RB and MD contributed to the acquisition of the financial supports and resources leading to this publication. CSM, NC, MD, MG, AC, GJ, FDB, SL, RB and MD wrote the article, including

374 drafting and revising critically the manuscript for important intellectual content. All authors
375 have declared no competing interests.

References

1. Fairbrother, J. M. & Nadeau, É. *Escherichia coli*: On-farm contamination of animals. *OIE Rev. Sci. Tech.* **25**, 555–569 (2006).

2. Kintz, E., Brainard, J., Hooper, L. & Hunter, P. Transmission pathways for sporadic Shiga-toxin producing *E. coli* infections: A systematic review and meta-analysis. *Int. J. Hyg. Environ. Health* **220**, 57–67 (2017).

3. Fremaux, B., Prigent-Combaret, C. & Vernozy-Rozand, C. Long-term survival of Shiga toxin-producing *Escherichia coli* in cattle effluents and environment: an updated review. *Vet. Microbiol.* **132**, 1–18 (2008).

4. Jackson, T. C., Hardin, M. D. & Acuff, G. R. Heat resistance of *Escherichia coli* O157:H7 in a nutrient medium and in ground beef patties as influenced by storage and holding temperatures. *J. Food Prot.* **59**, 230–237 (1996).

5. The European Union One Health 2019 Zoonoses Report. *EFSA J.* **19**, (2021).

6. Kaper, J. B., Nataro, J. P. & Mobley, H. L. T. Pathogenic *Escherichia coli*. *Nat. Rev. Microbiol. 2004 22* **2**, 123–140 (2004).

7. Delignette-Muller, M. L. & Cornu, M. Quantitative risk assessment for *Escherichia coli* O157:H7 in frozen ground beef patties consumed by young children in French households. *Int. J. Food Microbiol.* **128**, 158–164 (2008).

8. Devleesschauwer, B., Pires, S. M., Young, I., Gill, A. & Majowicz, S. E. Associating sporadic, foodborne illness caused by Shiga toxin-producing *Escherichia coli* with specific foods: a systematic review and meta-analysis of case-control studies. *Epidemiol. Infect.* **147**, (2019).

9. Lobete, M. M., Fernandez, E. N. & Van Impe, J. F. M. Recent trends in non-invasive in situ techniques to monitor bacterial colonies in solid (model) food. *Frontiers in Microbiology* vol. 6 (2015).

10. Schröter, L. & Dersch, P. Phenotypic Diversification of Microbial Pathogens—Cooperating and Preparing for the Future. *Journal of Molecular Biology* vol. 431 4645–4655 (2019).

404 11. Stewart, P. S. & Franklin, M. J. Physiological heterogeneity in biofilms. *Nature*
405 *Reviews Microbiology* vol. 6 199–210 (2008).

406 12. Rantsiou, K., Mataragas, M., Alessandria, V. & Cocolin, L. Expression of virulence
407 genes of *Listeria monocytogenes* in food. *J. Food Saf.* **32**, 161–168 (2012).

408 13. Costello, K. M. *et al.* Modelling the microbial dynamics and antimicrobial resistance
409 development of Listeria in viscoelastic food model systems of various structural
410 complexities. *Int. J. Food Microbiol.* **286**, 15–30 (2018).

411 14. Rowbury, R. J. & Goodson, M. Extracellular sensing and signalling pheromones
412 switch-on thermotolerance and other stress responses in *Escherichia coli*. *Sci. Prog.* **84**,
413 205–233 (2001).

414 15. Bhattacharjee, T. & Datta, S. S. Bacterial hopping and trapping in porous media. *Nat.*
415 *Commun.* **10**, (2019).

416 16. Antwi, M. *et al.* Influence of a gel microstructure as modified by gelatin concentration
417 on Listeria innocua growth. *Innov. Food Sci. Emerg. Technol.* **7**, 124–131 (2006).

418 17. Kabanova, N., Stulova, I. & Vilu, R. Microcalorimetric study of the growth of bacterial
419 colonies of Lactococcus lactis IL1403 in agar gels. *Food Microbiol.* **29**, 67–79 (2012).

420 18. Skandamis, P. N. & Jeanson, S. Colonial vs. planktonic type of growth: Mathematical
421 modeling of microbial dynamics on surfaces and in liquid, semi-liquid and solid foods.
422 *Frontiers in Microbiology* vol. 6 (2015).

423 19. Antwi, M., Bernaerts, K., Van Impe, J. F. & Geeraerd, A. H. Modelling the combined
424 effects of structured food model system and lactic acid on Listeria innocua and
425 Lactococcus lactis growth in mono- and coculture. *Int. J. Food Microbiol.* **120**, 71–84
426 (2007).

427 20. Smith, D. K., Kassam, T., Singh, B. & Elliott, J. F. *Escherichia coli* has two
428 homologous glutamate decarboxylase genes that map to distinct loci. *J. Bacteriol.* **174**,
429 5820–5826 (1992).

430 21. Cotter, P. D., Gahan, C. G. M. & Hill, C. A glutamate decarboxylase system protects
431 *Listeria monocytogenes* in gastric fluid. *Mol. Microbiol.* **40**, 465–475 (2001).

22. Nomura, M. *et al.* Lactococcus lactis contains only one glutamate decarboxylase gene. *Microbiology* **145**, 1375–1380 (1999).

23. Waterman, S. R. & Small, P. L. C. The glutamate-dependent acid resistance system of *Escherichia coli* and Shigella flexneri is inhibited in vitro by l-trans-pyrrolidine-2,4-dicarboxylic acid. *FEMS Microbiol. Lett.* **224**, 119–125 (2003).

24. Waterman, S. R. & Small, P. L. C. Transcriptional expression of *Escherichia coli* glutamate-dependent acid resistance genes *gadA* and *gadBC* in an hns rpoS mutant. *J. Bacteriol.* **185**, 4644–4647 (2003).

25. Capitani, G. *et al.* Crystal structure and functional analysis of *Escherichia coli* glutamate decarboxylase. *EMBO J.* **22**, 4027–4037 (2003).

26. De Biase, D., Tramonti, A., Bossa, F. & Visca, P. The response to stationary-phase stress conditions in *Escherichia coli*: Role and regulation of the glutamic acid decarboxylase system. *Mol. Microbiol.* **32**, 1198–1211 (1999).

27. De Roy, K., Marzorati, M., Van den Abbeele, P., Van de Wiele, T. & Boon, N. Synthetic microbial ecosystems: an exciting tool to understand and apply microbial communities. *Environ. Microbiol.* **16**, 1472–1481 (2014).

28. Verheyen, D. *et al.* Food microstructure and fat content affect growth morphology, growth kinetics, and preferred phase for cell growth of *Listeria monocytogenes* in fish-based model systems. *Appl. Environ. Microbiol.* **85**, (2019).

29. Saint Martin, C. *et al.* Spatial organisation of *Listeria monocytogenes* and *Escherichia coli* O157:H7 cultivated in gel matrices. *Food Microbiol.* **103**, 103965 (2022).

30. Gobert, A. P. *et al.* Shiga Toxin Produced by Enterohemorrhagic *Escherichia coli* Inhibits PI3K/NF-κB Signaling Pathway in Globotriaosylceramide-3-Negative Human Intestinal Epithelial Cells. *J. Immunol.* **178**, 8168–8174 (2007).

31. Chagnot, C. *et al.* Colonization of the meat extracellular matrix proteins by O157 and non-O157 enterohemorrhagic *Escherichia coli*. *Int. J. Food Microbiol.* **188**, 92–98 (2014).

32. Graveline, R. *et al*. Monitoring F1651 P-like fimbria expression at the single-cell level reveals a highly heterogeneous phenotype. *Infect. Immun.* **83**, 1929–1939 (2015).

461 33. Lim, H. N. & Van Oudenaarden, A. A multistep epigenetic switch enables the stable
462 inheritance of DNA methylation states. *Nat. Genet.* **39**, 269–275 (2007).

463 34. Datsenko, K. A. & Wanner, B. L. One-step inactivation of chromosomal genes in
464 *Escherichia coli* K-12 using PCR products. *Proc. Natl. Acad. Sci. U. S. A.* **97**, 6640–
465 6645 (2000).

466 35. Hartmann, R. *et al*. Quantitative image analysis of microbial communities with
467 BiofilmQ. *Nat. Microbiol.* **6**, 151–156 (2021).

468 36. Pin, C., Sutherland, J. P. & Baranyi, J. Validating predictive models of food spoilage
469 organisms. *J. Appl. Microbiol.* **87**, 491–499 (1999).

470 37. Smith, S. & Schaffner, D. W. Evaluation of a Clostridium perfringens predictive
471 model, developed under isothermal conditions in broth, to predict growth in ground
472 beef during cooling. *Appl. Environ. Microbiol.* **70**, 2728–2733 (2004).

473 38. Baka, M., Noriega, E., Van Langendonck, K. & Van Impe, J. F. Influence of food
474 intrinsic complexity on *Listeria monocytogenes* growth in/on vacuum-packed model
475 systems at suboptimal temperatures. *Int. J. Food Microbiol.* **235**, 17–27 (2016).

476 39. Baka, M., Verheyen, D., Cornette, N., Vercruyssen, S. & Van Impe, J. F. Salmonella
477 Typhimurium and Staphylococcus aureus dynamics in/on variable (micro)structures of
478 fish-based model systems at suboptimal temperatures. *Int. J. Food Microbiol.* **240**, 32–
479 39 (2017).

480 40. Baka, M., Vercruyssen, S., Cornette, N. & Van Impe, J. F. Dynamics of *Listeria*
481 *monocytogenes* at suboptimal temperatures in/on fish-protein based model systems:
482 Effect of (micro)structure and microbial distribution. *Food Control* **73**, 43–50 (2017).

483 41. Bury-Moné, S. & Sclavi, B. Stochasticity of gene expression as a motor of epigenetics
484 in bacteria: from individual to collective behaviors. *Research in Microbiology* vol. 168
485 503–514 (2017).

486 42. Caniça, M., Manageiro, V., Abriouel, H., Moran-Gilad, J. & Franz, C. M. A. P.
487 Antibiotic resistance in foodborne bacteria. *Trends in Food Science and Technology*
488 vol. 84 41–44 (2019).

489 43. Nielsen, M. B., Knudsen, G. M., Danino-Appleton, V., Olsen, J. E. & Thomsen, L. E.
490 Comparison of heat stress responses of immobilized and planktonic Salmonella
491 enterica serovar Typhimurium. *Food Microbiol.* **33**, 221–227 (2013).

492 44. Su, L. K. *et al.* Lysogenic infection of a Shiga toxin 2-converting bacteriophage
493 changes host gene expression, enhances host acid resistance and motility. *Mol. Biol.* **44**,
494 54–66 (2010).

495 45. Cinquin, B. & Lopes, F. Structure and fluorescence intensity measurements in biofilms.
496 in *Methods in Molecular Biology* vol. 2040 117–133 (Humana Press Inc., 2019).

497 46. Lenz, A. P., Williamson, K. S., Pitts, B., Stewart, P. S. & Franklin, M. J. Localized
498 gene expression in Pseudomonas aeruginosa biofilms. *Appl. Environ. Microbiol.* **74**,
499 4463–4471 (2008).

500 47. Floyd, K. A. *et al.* Adhesive Fiber Stratification in Uropathogenic *Escherichia coli*
501 Biofilms Unveils Oxygen-Mediated Control of Type 1 Pili. *PLOS Pathog.* **11**,
502 e1004697 (2015).

503 48. Klauck, G., Serra, D. O., Possling, A. & Hengge, R. Spatial organization of different
504 sigma factor activities and c-di-GMP signalling within the three-dimensional landscape
505 of a bacterial biofilm. *Open Biol.* **8**, (2018).

506 49. Ross, T. & McMeekin, T. A. Modeling Microbial Growth Within Food Safety Risk
507 Assessments. *Risk Anal.* **23**, 179–197 (2003).

508 50. Hernández-Galán, L. *et al.* Effect of dairy matrices on the survival of Streptococcus
509 thermophilus, Brevibacterium aurantiacum and Hafnia alvei during digestion. *Food*
510 *Res. Int.* **100**, 477–488 (2017).

511 51. Heumann, A. *et al.* Intestinal release of biofilm-like microcolonies encased in calcium-
512 pectinate beads increases probiotic properties of Lacticaseibacillus paracasei. *npj*
513 *Biofilms Microbiomes 2020 61* **6**, 1–12 (2020).

514 52. Chamignon, C. *et al.* Evaluation of the Probiotic Properties and the Capacity to Form
515 Biofilms of Various Lactobacillus Strains. *Microorg. 2020, Vol. 8, Page 1053* **8**, 1053
516 (2020).

517 53. Lee, J. *et al.* Structure and Function of the *Escherichia coli* Protein YmgB: A Protein
518 Critical for Biofilm Formation and Acid-resistance. *J. Mol. Biol.* **373**, 11–26 (2007).

519 54. Wood, T. K. Insights on *Escherichia coli* biofilm formation and inhibition from whole-
520 transcriptome profiling. *Environmental Microbiology* vol. 11 1–15 (2009).

521 55. Jeong, K. C., Hung, K. F., Baumler, D. J., Byrd, J. J. & Kaspar, C. W. Acid stress
522 damage of DNA is prevented by Dps binding in *Escherichia coli* O157:H7. *BMC*
523 *Microbiol.* **8**, 1–13 (2008).

524 56. Sang Ho Choi, Baumler, D. J. & Kaspar, C. W. Contribution of dps to acid stress
525 tolerance and oxidative stress tolerance in *Escherichia coli* O157:H7. *Appl. Environ.*
526 *Microbiol.* **66**, 3911–3916 (2000).

Supplementary materials

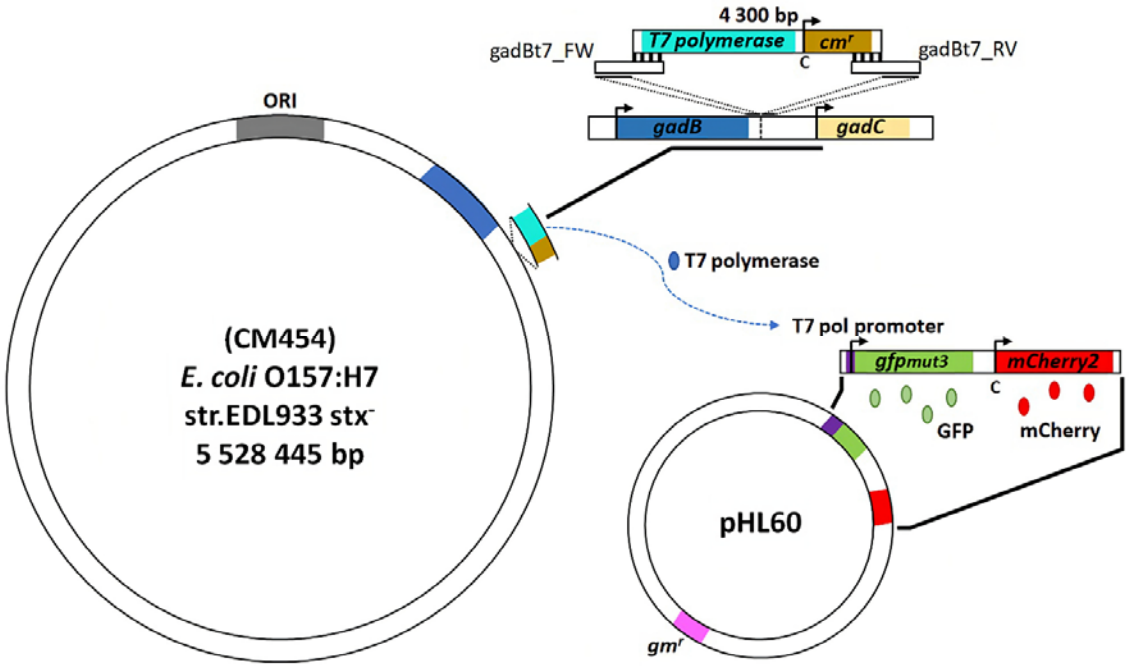

Figure S1: Strategy of the genetic constructions. (A) chromosome of *E. coli* O157:H7 with a zoom on the region of the insert and how the different CDS are present in this situation. The cassette bearing the *T7 polymerase* (in turquoise) and resistance gene cm^r (in brown) is elongated by PCR with two primers (gadBt7_FW and gadBt7_RV) so that a homology sequence exists with insertion site. This site is located between the gene interest *gadB* (in blue) and *gadC* (in yellow). On the right the low copy plasmid pHL60 bearing the fluorophore encoding genes is represented. It contains the constitutively expressed *mCherry2* (in red) sequence and *gfpmut3* (in green) under the control of the *T7 pol promoter* (in purple), as well as a gentamicin resistance gene gm^r (in pink).

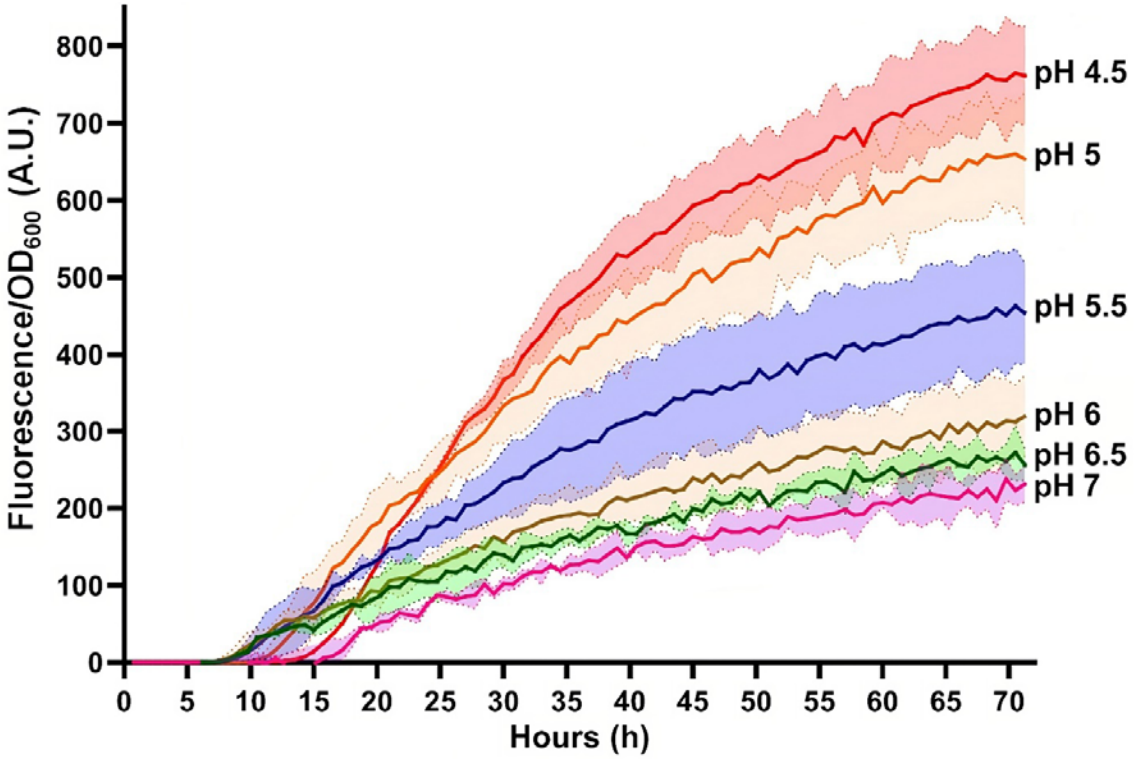

Figure S2: Relative expression of *gadB* in a population in function of time and under different acidity levels. The fluorescence of planktonic populations of *E. coli* O157:H7 *gadB::GFP* are represented in function of the OD_{600}. For each curve representing the mean signal over time, the standard deviation of values is shown as an area of lighter color. These curves show that detected fluorescence becomes incrementally brighter with decreasing pHs. The rise in expressed fluorescence is not linear with greater leaps of intensity below pH=6.0. Points over time show that fluorescence intensity at pH 4.5 can be 3-4 times higher than reported values for the pH=7.0 control. The lag time before the green fluorescence is detected is high at pH 7.0 (15 hours) compared to pH=5.5 where it starts after eight hours. In media pH=5.0 and pH=4.5, the lag time becomes progressively longer (12 then 14 hours).

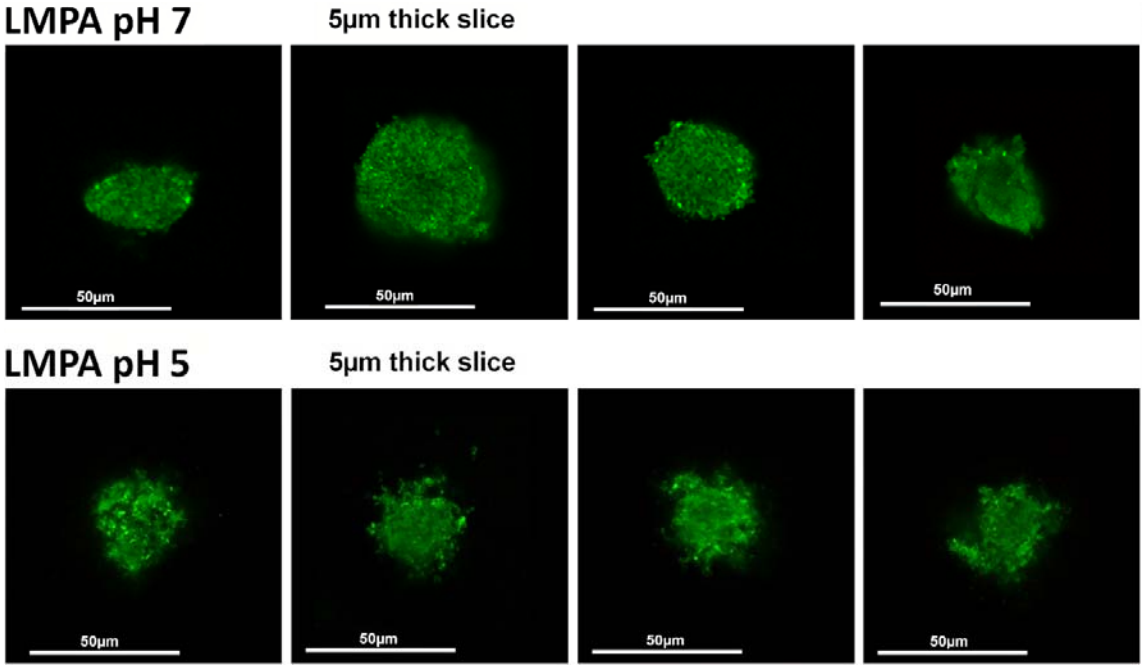

Figure S3: Qualitative presentation of the constitutive GFP spatial expression in microcolonies at pH=7 or pH=5. A control group with a constitutive GFP to verify that at pH=7 (up) and/or pH=5 (down) the fluorescence of the green fluorescence is not already spatialized. Each image is a 5µm slice of a stack.

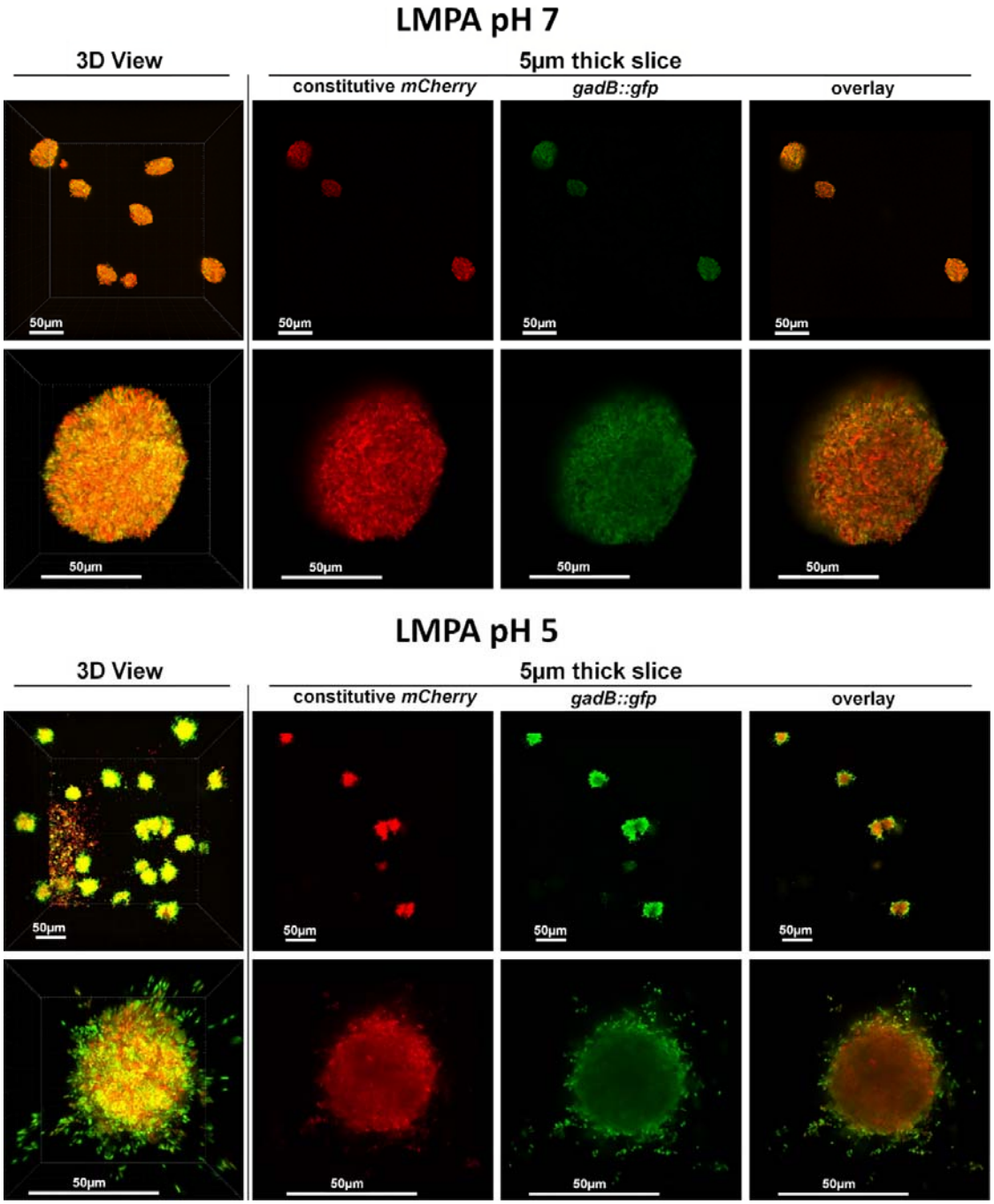

Figure S4: Qualitative presentation of *gadB* spatial expression in microcolonies at pH=7 or pH=5. Microscopic observations of the expression of *gadB* in the control LMPA pH=7 (top) and in the acid matrix LMPA pH=5 (bottom). For both groups, the 2 successive rows use a 40X then a 63X objective to present a collection of microcolonies and a close observation of a single example. Each image is shown as a 3-dimensional representation (leftmost column) and in each case a series of 5 µm slices show both fluorescent channels (middles columns) and the overlay (Rightmost column). The first row of each condition was

taken with a 40x air objective (numerical aperture = 0.85) to explore a 290 µm x 290 µm fields.

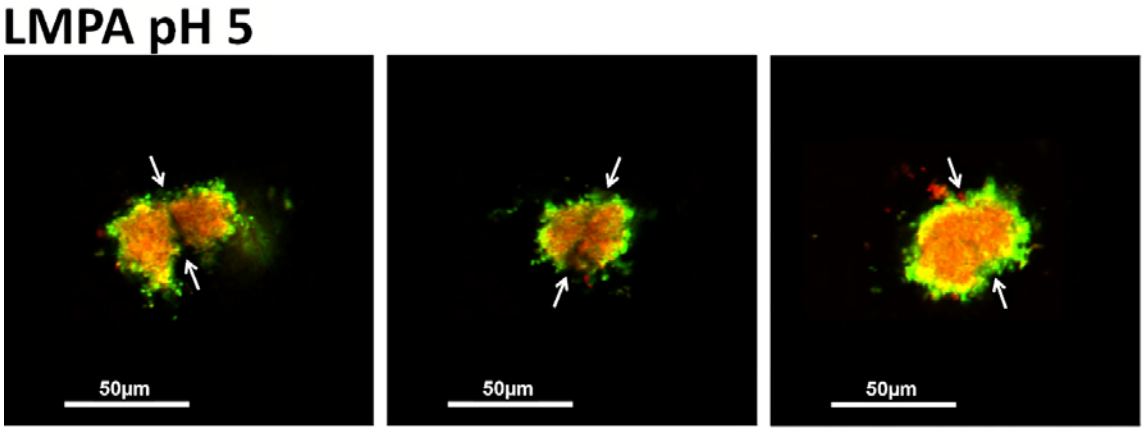

Figure S5: The case of joint microcolonies. Examples where two microcolonies of *E. coli* O157:H7 are touching or merging in LMPA pH=5. White arrows indicate the separation between each microcolonies.

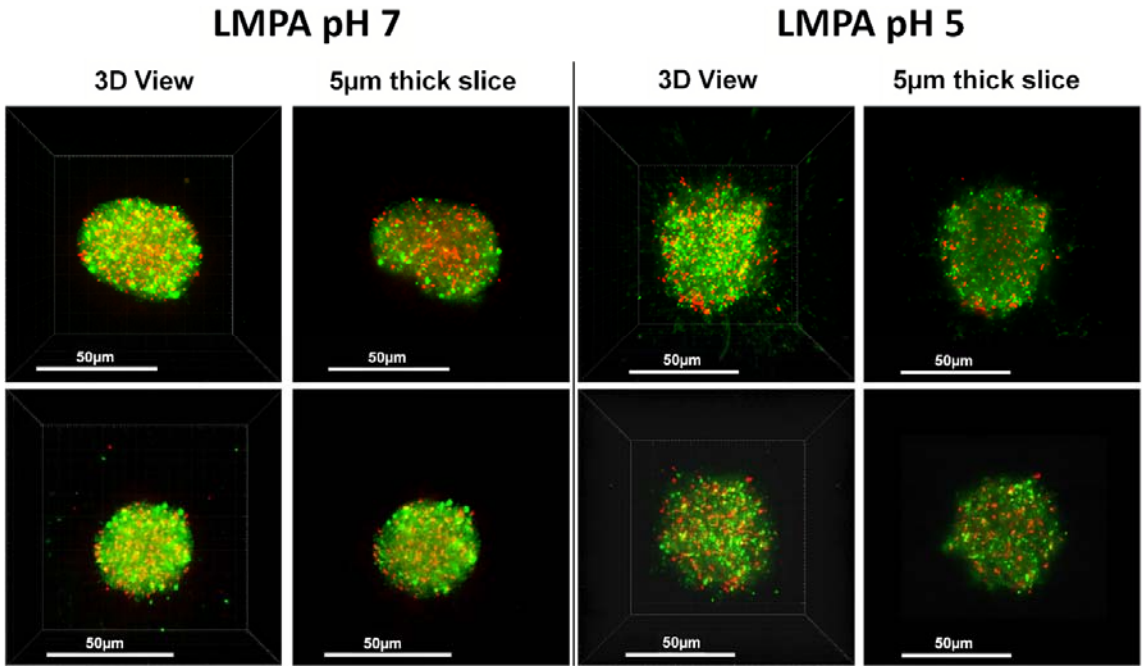

Figure S6: Live/Dead staining in the gel microcolonies. Bacterial cells in microcolonies grown in neutral (left side) or acidic (right side) were labeled with the cell impermeant propidium iodine (red, dead cells) and the cell permeant SYTO 9 (Green, all cells).